Supplementary information for:

Isomeric lipid signatures reveal compartmentalised fatty acid metabolism in cancer

Reuben S. E. Young[1,4], Andrew P. Bowman[2], Kaylyn D. Tousignant[3], Berwyck L. J. Poad[1,4], Jennifer H. Gunter[3], Lisa K. Philp[3], Colleen C. Nelson[3], Shane R. Ellis[2,5,6], Ron M. A. Heeren[2], Martin C. Sadowski[3,7]* & Stephen J. Blanksby[1,4]*.

Affiliations

[1]School of Chemistry and Physics, Queensland University of Technology, Brisbane, QLD 4000, Australia.
[2]M4I, The Maastricht MultiModal Molecular Imaging Institute, Division of Imaging Mass Spectrometry, Maastricht University, Universiteitssingel 50, 6229 ER Maastricht, The Netherlands.
[3]Australian Prostate Cancer Research Centre - Queensland, Institute of Health and Biomedical Innovation, School of Biomedical Sciences, Faculty of Health, Queensland University of Technology (QUT), Princess Alexandra Hospital, Translational Research Institute, Brisbane, QLD 4000, Australia.
[4]Central Analytical Research Facility, Queensland University of Technology, Brisbane, QLD 4000, Australia.
[5]Molecular Horizons and School of Chemistry and Molecular Bioscience, University of Wollongong, Wollongong, NSW 2522, Australia.
[6]Illawarra Health and Medical Research Institute (IHMRI), Wollongong, NSW 2522, Australia.
[7]Institute of Pathology, University of Bern, Murtenstrasse 31, CH-3008 Bern, Switzerland.

*Corresponding authors: stephen.blanksby@qut.edu.au
martin.sadowski@pathology.unibe.ch

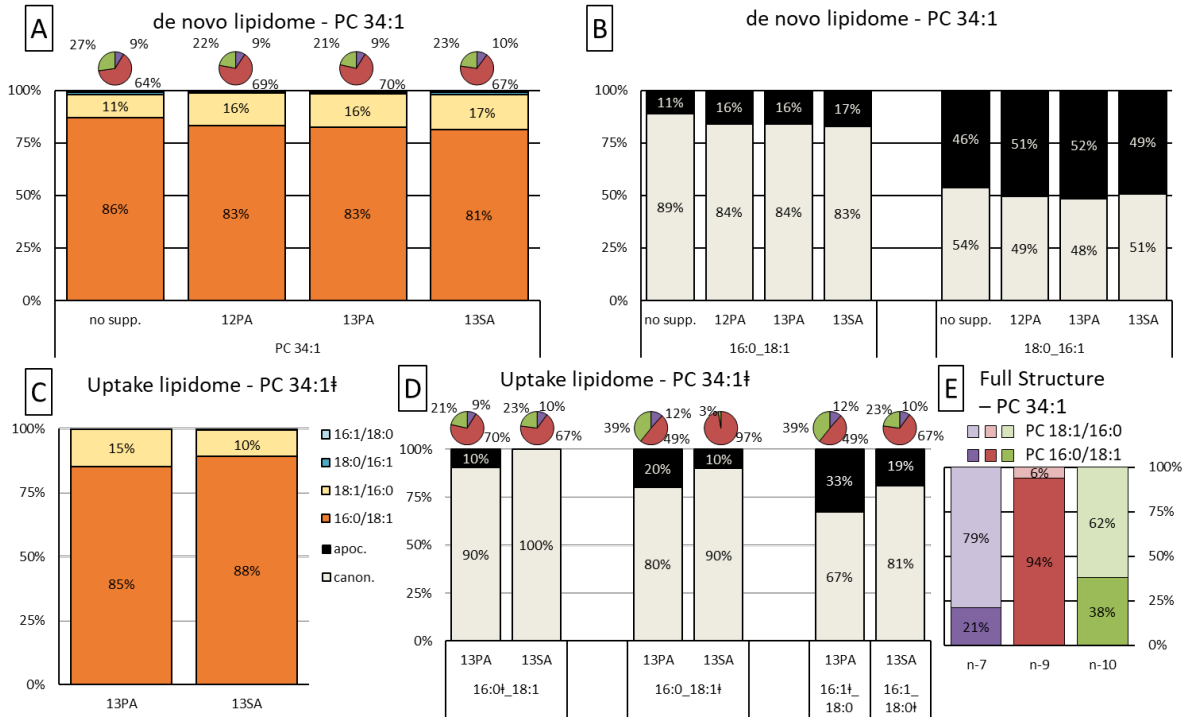

Fig. S1: (related to Fig. 2 & 3) *de novo* and *uptake* PC 34:1 DB and *sn*-isomer distributions for non-supplemented LNCaP, 12PA supplemented LNCaP, 13PA supplemented LNCaP and 13SA supplemented LNCaP.

(A) Relative abundance of FA compositions for *de novo* (unlabelled) PC 34:1, including *sn*- isomer distribution and DB locational isomer distribution (pie charts). **(B)** Relative abundance of *sn*- isomers for either *de novo* (unlabelled) FA composition of PC 34:1. **(C)** Relative abundance of FA compositions for *uptake* (labelled) PC 34:1, including *sn*- isomer distribution. **(D)** Relative abundance of *sn*- isomers for either *uptake* (labelled) FA composition of PC 34:1, including DB locational isomer distribution (pie charts). **(E)** Full structural elucidation of non-supplemented LNCaP PC 34:1, showing combined *sn*- and DB isomer distribution and the association between either type of isomer. Mean ± SEM (95% confidence interval), n = 2, except for all non-supplemented LNCaP data where n = 3. Isotope labelling is indicated with a double dagger (ǂ).

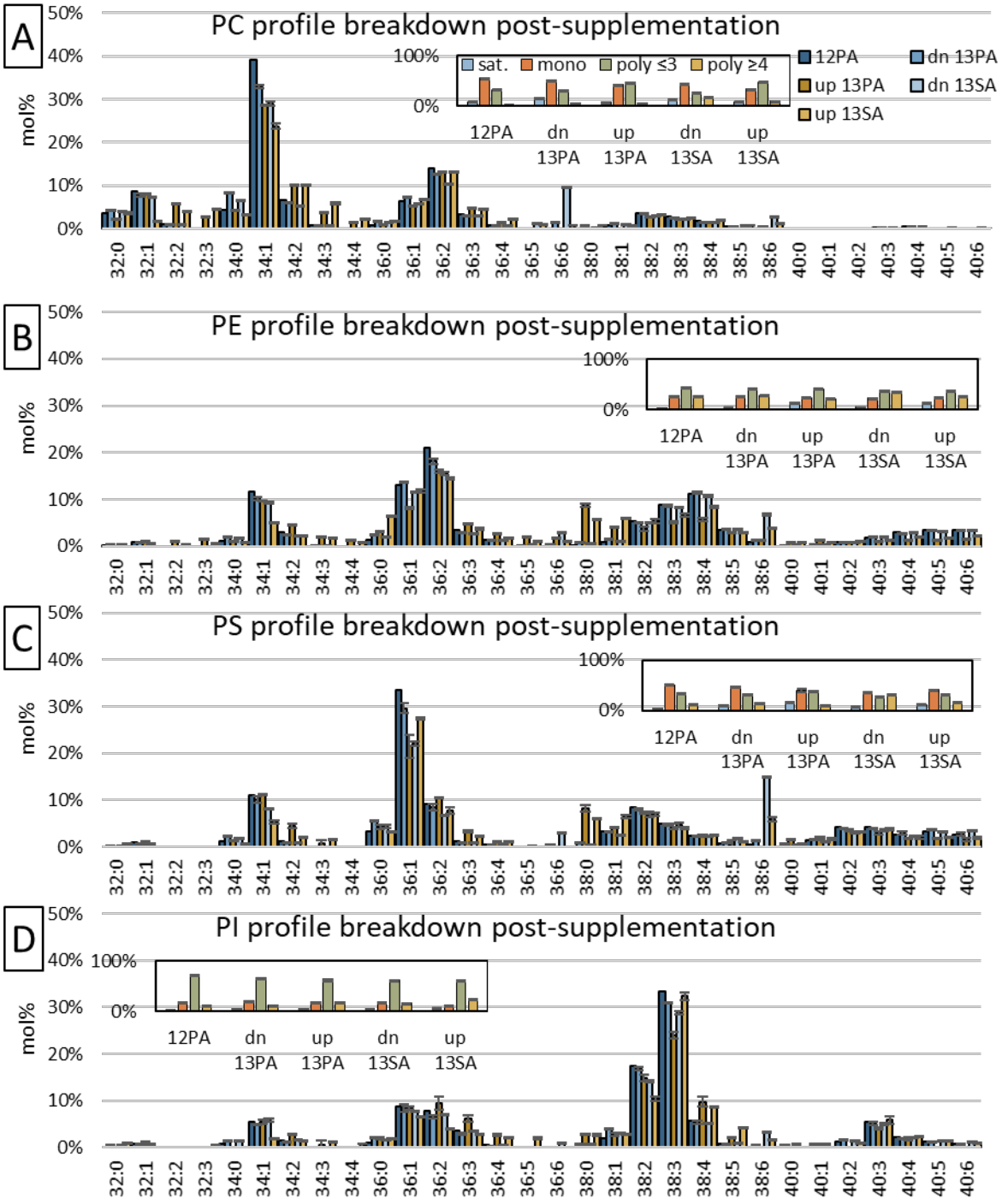

Fig. S2: (related to Fig. 1 & 4) Distribution of labelled fatty acids into GPL classes and their effect on species abundance and degree of unsaturation.

(A-D) Main bar charts show the species abundance (mol%) for PC, PE, PS and PI and the impact labelled fatty acid supplements indirectly have on the unlabelled lipidome and directly have on the labelled lipidome. Smaller bar charts show the impact supplements have on the degree of saturation for each lipid class. Degree of unsaturation was divided into lipid species that contained fatty acids that were: saturated, monounsaturated, polyunsaturated (≤3 DBs) and polyunsaturated (≥4 DBs). Legends are located in panel A; n=2, mean ± SEM (95% confidence interval) displayed.

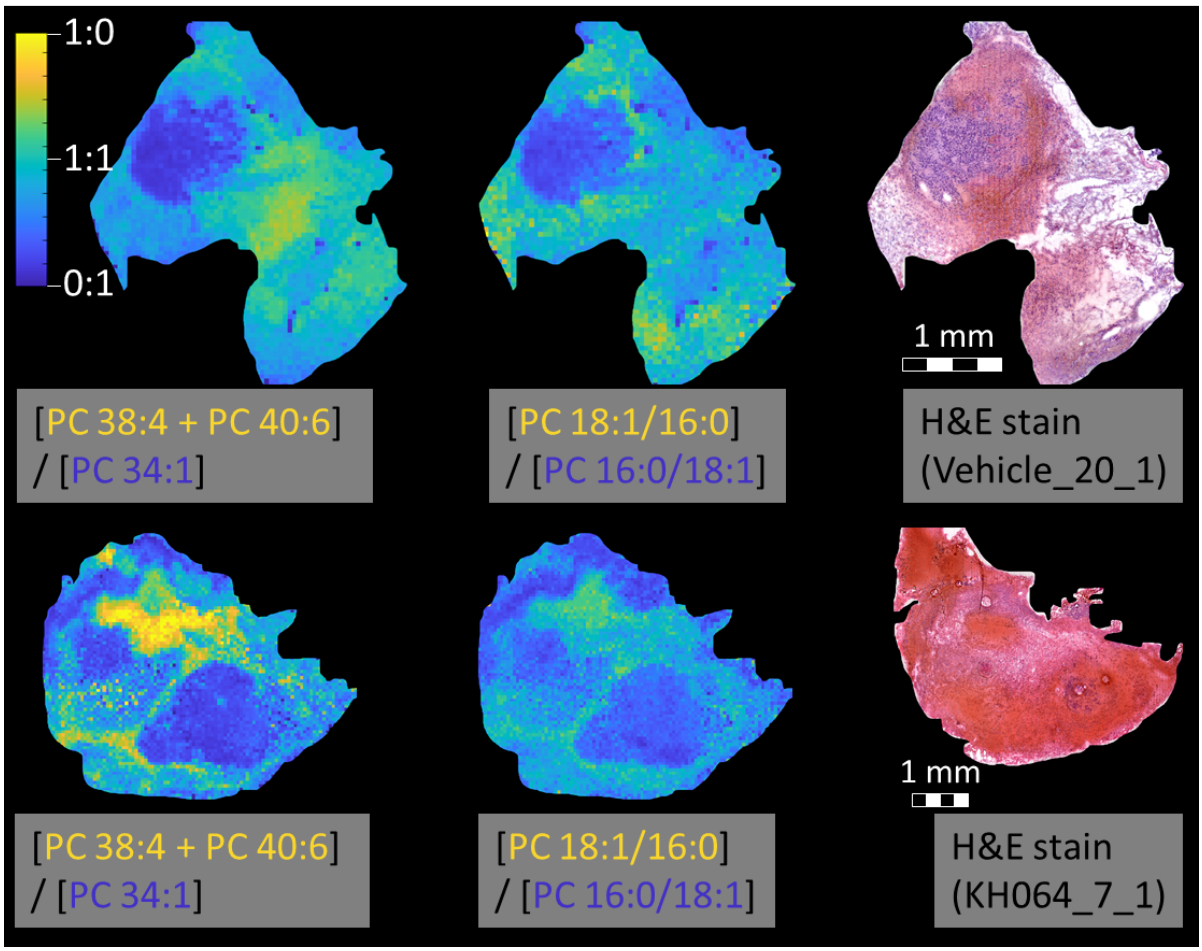

Fig. S3: (related to Fig. 5) Uninhibited LNCaP xenograft tissue (biological replicate) and $sPLA_2$-IIA inhibited (KH064) LNCaP xenograft tissue.

(Top row) Uninhibited (vehicle/treatment-naïve) LNCaP xenograft tissue showing the fractional distribution images (FDI) for PUFA containing PCs and canonomer/apocromer distribution across the tissue. As per the main text figure, positive correlation can be observed between the PUFA species, the PC 18:1/16:0 apocromer and the fatty tissue. **(Bottom row)** As per top row for the KH064 treated xenograft model. An increased abundance of PUFA lipid and decreased abundance of apocromer can be observed across the tissue. Although spatial correlation is still apparent, these changes to lipid species abundance thereby reduces the correlation between either species. Both still appear to be positively correlated with host adipocyte cells. Due to a sampling malfunction, directly adjacent tissue sections could not be analysed, instead the H&E displayed is 3-4 section depths (~30-40 µm) distal to the MALDI-MSI images.

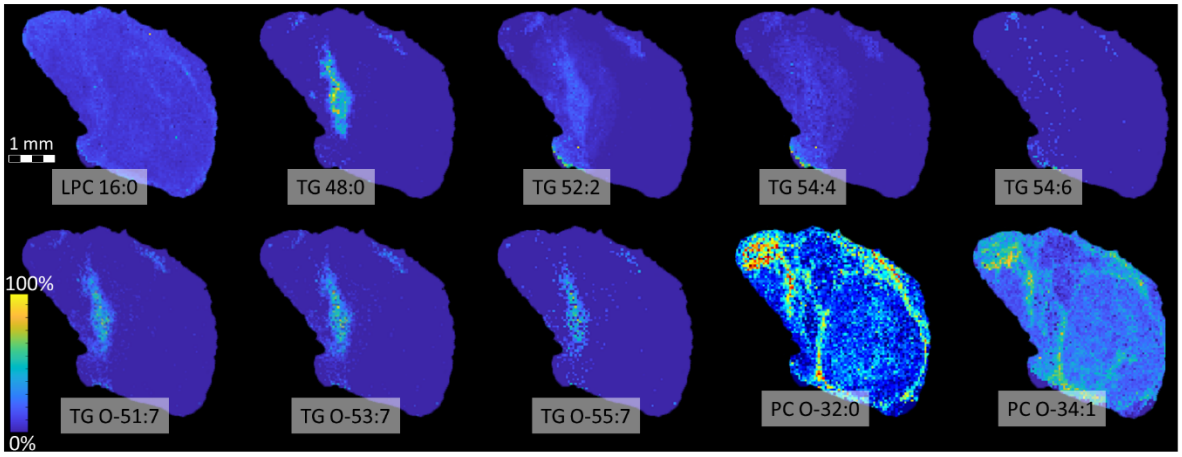

Fig. S4: (related to Fig. 5) Ether lipid species present in the uninhibited xenograft tissue.
Top row: Distribution and abundance differences of LPC 16:0 and triacylglycerol lipids.
Bottom row: Triacylglycerol ethers (TG O-) and phosphatidylcholine ethers (PC O-) were also observed to be spatially correlated to host adipocyte cells, PUFA lipids and increased apocromer abundance (H&E stain). While TG O- appears mostly homogenous across the region, PC O- appears to be more abundant around the perimeter. All species were identified by exact mass (Δppm ≤ 3), with no reasonable alternative identifications found using LIPID MAPS® or other lipid databases. Phosphatidylethanolamine ethers (PE O-) were also potentially identified but were not included due to their isobaric overlap with $[PC + K]^+$ precursor ions. All high mass-resolution MALD-MSI images are normalised to self, displaying zero abundance (dark blue) ranging through to highest abundance (orange/red).